arXiv:nucl-th/0207031v1 11 Jul 2002

Cascade production from antikaon induced reactions on lambda and sigma

C. H. Li and C. M. Ko
Cyclotron Institute and Physics Department, Texas A&M University, College Station, Texas 77843

Using a gauged flavor SU(3) invariant hadronic Lagrangian, we study Ξ production from $\bar{K}$ induced reactions on Λ and Σ in a coupled-channel approach. Including the four channels of $\bar{K}\Lambda$, $\bar{K}\Sigma$, $\pi\Xi$, and $\eta\Xi$, we solve the Bethe-Salpeter equation in the K-matrix approximation by neglecting the off-shell contribution in the intermediate states. For the transition potential which drives the higher-order contribution, we consider all allowed Born diagrams in the s, t, and u channels. With coupling constants determined from the SU(3) symmetry with empirical input, we find that the cross sections for the reactions $\bar{K}\Lambda \to \pi\Xi$, $\bar{K}\Sigma \to \pi\Xi$, $\bar{K}\Lambda \to \eta\Xi$, and $\bar{K}\Sigma \to \eta\Xi$ all have values of a few mb. In contrast to the results from the lowest-order Born approximation, the magnitude of these cross sections is less sensitive to the values of the cut-off parameters in the form factors. From the transition matrix in the coupled-channel approach, we have further evaluated the cross sections for the elastic process $\bar{K}\Lambda \to \bar{K}\Lambda$, $\bar{K}\Sigma \to \bar{K}\Sigma$, $\pi\Xi \to \pi\Xi$, and $\eta\Xi \to \eta\Xi$ as well as for the inelastic processes $\bar{K}\Lambda \to \bar{K}\Sigma$ and $\pi\Xi \to \eta\Xi$. Implications of the reactions studied here in Ξ production from relativistic heavy ion collisions are discussed.

PACS number(s): 13.75.Jz

I. INTRODUCTION

Because of the large production rate of strange quarks in a quark-gluon plasma, enhanced production of hadrons consisting of multistrange quarks has been suggested as a possible signal for the quark-gluon plasma that is expected to be formed in relativistic heavy ion collisions [1]. However, multistrange hadrons can also be produced from the hadronic matter that dominates the later stage of heavy ion collisions. In particular, the strangeness-exchange reactions between antikaons and baryons, such as $\bar{K}N \to M\Lambda$, $\bar{K}N \to M\Sigma$, $\bar{K}\Lambda \to M\Xi$, $\bar{K}\Sigma \to M\Xi$, and $\bar{K}\Xi \to M\Omega$ with M denoting either pion or eta meson, have been shown in a multiphase transport model [2] to contribute significantly to the production of multistrange baryons such as Ξ and Ω [3]. Among these reactions, only the cross sections for $\bar{K}N \to \pi\Lambda$ and $\bar{K}N \to \pi\Sigma$ have been measured in experiments [4,5]. In Ref. [3], the cross sections for other processes are determined by assuming that they have the same transition matrix elements as that for the empirically measured reaction $\bar{K}N \to \pi\Sigma$.

To check the validity of the above assumption, we have evaluated using the coupled-channel approach the cross sections for Ξ production from the strangeness-exchange reactions induced by $\bar{K}$ on Λ and Σ. The interaction Lagrangians needed for this study are taken from a gauged flavor SU(3) invariant hadronic Lagrangian with empirical hadron masses. In Refs. [6–8], the same Lagrangian based on the SU(4) flavor symmetry has been used to study reactions involving vector mesons and pseudoscalar mesons. Here, we extend it to include the octet baryons. A Lagrangian similar to ours has been used in Refs. [9,10] to study the empirically known cross sections for the reactions $\bar{K}N \to \pi\Lambda$ and $\bar{K}N \to \pi\Sigma$. Solving the coupled-channel Bethe-Salpeter equation [11] for the transition matrix, it has been found that the measured cross sections can be reproduced with appropriate form factors at the interaction vertices. In the present study, we extend the method of Refs. [10,12], which includes only the on-shell part of the propagator in the Bethe-Salpeter equation but otherwise satisfies the unitarity condition, to study the strangeness-exchange reactions for Ξ production, i.e., $\bar{K}\Lambda \to M\Xi$ and $\bar{K}\Sigma \to M\Xi$ with M denoting either pion or eta meson.

This paper is organized as follows. In Section II, we introduce the hadronic model used for present study. In particular, the interaction Lagrangians that are relevant to Ξ production are derived from a gauged flavor SU(3) invariant Lagrangian with empirical hadron masses. Values of the coupling constants are then determined from the SU(3) symmetry with empirical input. The coupled-channel method is introduced in Section III. To solve the resulting Bethe-Salpeter equation for the transition matrix, the lowest-order Born diagrams are evaluated to construct the transition potential that drives the higher-order contributions, and the K-matrix approximation is used to reduce the Bethe-Salpeter equation to a simple form. In Section IV, details of our calculations are given. These include the transformation of the covariant transition matrix between the Dirac spinors to a transition matrix between Pauli spinors, and the partial wave expansion of the transition amplitude. Results on both the total and differential cross sections are given in Section V. We include not only results on the strangeness-exchange reactions for Ξ production but also those on the elastic and inelastic processes. We further compare and discuss the results obtained from the coupled-channel approach with those from the Born approximation. Finally, conclusions are given in Section VI. In the Appendix, we give the explicit expressions of the transition amplitudes for all Born diagrams included in present study.

II. THE HADRONIC MODEL

In this section, we introduce the Lagrangian based on the gauged flavor SU(3) symmetry for describing the interactions between mesons and baryons. Since the SU(3) symmetry is explicitly broken by the appreciable differences in hadron masses, the empirical hadron masses are used in the Lagrangian. For the coupling constants, we shall determine them using the SU(3) symmetry in terms of empirically known coupling constants.

A. The Lagrangian

The SU(3) invariant Lagrangian for octet pseudoscalar mesons and baryons interacting through pseudovector couplings can be written as

$$\begin{aligned} \mathcal{L} &= i\mathrm{Tr}(\bar{B}\partial\!\!\!/ B) + \mathrm{Tr}[(\partial_\mu P^\dagger)(\partial^\mu P)] + g' \left\{\mathrm{Tr}[(1-\alpha) \right. \\ &\times \left. \bar{B}\gamma^5\gamma^\mu B\partial_\mu P + (1+\alpha)(\partial_\mu P)\bar{B}\gamma^5\gamma^\mu B]\right\}, \end{aligned} \tag{1}$$

where P and B denote, respectively, the 3×3 matrix representations of pseudoscalar mesons and baryons, i.e.,

$$B = \begin{pmatrix} \frac{\Sigma^0}{\sqrt{2}} + \frac{\Lambda}{\sqrt{6}} & \Sigma^+ & p \\ \Sigma^- & -\frac{\Sigma^0}{\sqrt{2}} + \frac{\Lambda}{\sqrt{6}} & n \\ \Xi^- & \Xi^0 & -\sqrt{\frac{2}{3}}\Lambda \end{pmatrix}, \tag{2}$$

$$P = \frac{1}{\sqrt{2}} \begin{pmatrix} \frac{\pi^0}{\sqrt{2}} + \frac{\eta_8}{\sqrt{6}} + \frac{\eta_0}{\sqrt{3}} & \pi^+ & K^+ \\ \pi^- & -\frac{\pi^0}{\sqrt{2}} + \frac{\eta_8}{\sqrt{6}} + \frac{\eta_0}{\sqrt{3}} & K^0 \\ K^- & \bar{K}^0 & -\sqrt{\frac{2}{3}}\eta_8 + \frac{\eta_0}{\sqrt{3}} \end{pmatrix}. \tag{3}$$

In Eq.(1), g' is the universal pseudovector coupling of pseudoscalar mesons to baryons, while the parameter α denotes the ratio of the F type coupling ($\mathrm{Tr}[(B\bar{B} + \bar{B}B)M]$) to the D type coupling ($\mathrm{Tr}[(B\bar{B} - \bar{B}B)M]$).

To include the interactions of baryons and pseudoscalar mesons with vector mesons, we treat vector mesons as gauge particles by replacing the partial derivative ∂_μ in Eq.(1) with the covariant derivative

$$D_\mu = \partial_\mu - \frac{i}{2}g[V_\mu,\ ], \tag{4}$$

where V denotes the matrix representation of vector mesons, i.e.,

$$V = \frac{1}{\sqrt{2}} \begin{pmatrix} \frac{\rho^0}{\sqrt{2}} + \frac{\omega}{\sqrt{2}} & \rho^+ & K^{*+} \\ \rho^- & -\frac{\rho^0}{\sqrt{2}} + \frac{\omega}{\sqrt{2}} & K^{*0} \\ K^{*-} & \bar{K}^{*0} & \phi \end{pmatrix}, \tag{5}$$

and g denotes the universal coupling of vector mesons with baryons and pseudoscalar mesons.

In Eq.(3), η_8 and η_0 are, respectively, the octet and singlet eta mesons, and they are mixtures of physical η and η', i.e.,

$$\eta_8 = \cos\theta\ \eta + \sin\theta\ \eta',\ \eta_0 = -\sin\theta\ \eta + \cos\theta\ \eta'. \tag{6}$$

The mixing angle θ is not well determined and has a value between -10° and -23° [13]. In the present study, we choose the mixing angle to be -23° but will study how our results change when it is taken to be -10°. Also, we shall consider only the η meson in the present study as the η' meson is more massive and will not contribute significantly to Ξ production from the strangeness-exchange reactions in a hadronic matter.

B. Interaction Lagrangians

Expanding the Lagrangian in Eq. (1) using the explicit matrix representations of P, V, and B, we obtain the following interaction Lagrangians that are relevant to Ξ production in strangeness-exchange reactions:

$$\begin{aligned}
\mathcal{L}_{\rho\pi\pi} &= g_{\rho\pi\pi}\vec{\pi}\cdot\partial_\mu\vec{\pi}\times\vec{\rho}^\mu, \\
\mathcal{L}_{\rho KK} &= -ig_{\rho KK}(\bar{K}\vec{\tau}\partial_\mu K - \partial_\mu\bar{K}\vec{\tau}K)\cdot\vec{\rho}^\mu, \\
\mathcal{L}_{\omega KK} &= -ig_{\omega KK}(\bar{K}\partial_\mu K - \partial_\mu\bar{K}K)\omega^\mu, \\
\mathcal{L}_{\phi KK} &= -ig_{\phi KK}(\bar{K}\partial_\mu K - \partial_\mu\bar{K}K)\phi^\mu, \\
\mathcal{L}_{K^*K\pi} &= -ig_{K^*K\pi}(\bar{K}\vec{\tau}K^{*\mu}\cdot\partial_\mu\vec{\pi} - \partial_\mu\bar{K}\vec{\tau}K^{*\mu}\cdot\vec{\pi}) \\
&\quad + \mathrm{H.c}, \\
\mathcal{L}_{K^*K\eta} &= -ig_{K^*K\eta}(\bar{K}K^{*\mu}\partial_\mu\eta - \partial_\mu\bar{K}K^{*\mu}\eta) + \mathrm{H.c}, \\
\mathcal{L}_{\pi\Lambda\Sigma} &= \frac{f_{\pi\Lambda\Sigma}}{m_\pi}\bar{\Lambda}\gamma^5\gamma^\mu\vec{\Sigma}\cdot\partial_\mu\vec{\pi} + \mathrm{H.c}, \\
\mathcal{L}_{\pi\Sigma\Sigma} &= i\frac{f_{\pi\Sigma\Sigma}}{m_\pi}\bar{\vec{\Sigma}}\gamma^5\gamma^\mu\cdot\vec{\Sigma}\times\partial_\mu\vec{\pi}, \\
\mathcal{L}_{\pi\Xi\Xi} &= \frac{f_{\pi\Xi\Xi}}{m_\pi}\bar{\Xi}\gamma^5\gamma^\mu\vec{\tau}\Xi\cdot\partial_\mu\vec{\pi}, \\
\mathcal{L}_{\eta\Lambda\Lambda} &= \frac{f_{\eta\Lambda\Lambda}}{m_\eta}\bar{\Lambda}\gamma^5\gamma^\mu\Lambda\partial_\mu\eta, \\
\mathcal{L}_{\eta\Sigma\Sigma} &= \frac{f_{\eta\Sigma\Sigma}}{m_\eta}\bar{\Sigma}\gamma^5\gamma^\mu\Sigma\partial_\mu\eta, \\
\mathcal{L}_{\eta\Xi\Xi} &= \frac{f_{\eta\Xi\Xi}}{m_\eta}\bar{\Xi}\gamma^5\gamma^\mu\Xi\partial_\mu\eta \\
\mathcal{L}_{KN\Lambda} &= \frac{f_{KN\Lambda}}{m_K}\bar{N}\gamma^5\gamma^\mu\Lambda\partial_\mu K + \mathrm{H.c.}, \\
\mathcal{L}_{KN\Sigma} &= \frac{f_{KN\Sigma}}{m_K}\bar{N}\gamma^5\gamma^\mu\vec{\tau}\cdot\vec{\Sigma}\partial_\mu K + \mathrm{H.c.}, \\
\mathcal{L}_{K\Lambda\Xi} &= \frac{f_{K\Lambda\Xi}}{m_K}\bar{\Xi}\gamma^5\gamma^\mu\Lambda\partial_\mu\bar{K}^T + \mathrm{H.c}, \\
\mathcal{L}_{K\Sigma\Xi} &= \frac{f_{K\Sigma\Xi}}{m_K}\bar{\Xi}\gamma^5\gamma^\mu\vec{\tau}\cdot\vec{\Sigma}\partial_\mu\bar{K}^T + \mathrm{H.c}, \\
\mathcal{L}_{\rho\Sigma\Sigma} &= ig_{\rho\Sigma\Sigma}\bar{\vec{\Sigma}}\gamma^\mu\cdot\vec{\Sigma}\times\vec{\rho}^\mu, \\
\mathcal{L}_{\rho\Xi\Xi} &= g_{\rho\Xi\Xi}\bar{\Xi}\gamma^\mu\vec{\tau}\Xi\cdot\vec{\rho}^\mu \\
\mathcal{L}_{K^*\Lambda\Xi} &= g_{K^*\Lambda\Xi}\bar{\Xi}\gamma^\mu\Lambda\bar{K}_\mu^{*T} + \mathrm{H.c}, \\
\mathcal{L}_{K^*\Sigma\Xi} &= g_{K^*\Sigma\Xi}\bar{\Xi}\gamma^\mu\vec{\tau}\cdot\vec{\Sigma}\bar{K}_\mu^{*T} + \mathrm{H.c},
\end{aligned} \tag{7}$$

In the above, $\vec{\tau}$ are Pauli matrices; $\vec{\pi}$, $\vec{\rho}$, and $\vec{\Sigma}$ denote the pion, rho meson, and sigma hyperon isospin triplets, respectively, with the usual phase convention of defining the positively charged states with an extra minus sign with respect to the isospin state $|I=1, I_z=1>$. Furthermore, $\bar{K}=(K^-, \bar{K}^0)$, and $\bar{K}^*=(K^{*-}, \bar{K}^{*0})$ denote the pseudoscalar and vector antikaon isospin doublets, respectively, and $\bar{\Xi}=(\bar{\Xi}^-, \bar{\Xi}^0)$ is the cascade hyperon isospin doublet.

In terms of the SU(3) coupling constants g, g', α, and the mixing angle θ, the hadronic coupling constants introduced in Eq.(7) can be expressed as

$$\begin{aligned}
&g_{\rho\pi\pi}=\frac{g}{4},\ g_{\rho KK}=-\frac{g}{4},\ g_{\omega KK}=-\frac{g}{4},\ g_{\phi KK}=\frac{g}{2\sqrt{2}},\\
&g_{K^*K\pi}=\frac{g}{4},\ g_{K^*K\eta}=\frac{\sqrt{3}}{4}\cos\theta\ g,\\
&g_{\rho\Sigma\Sigma}=-\frac{g}{2},\ g_{\rho\Xi\Xi}=-\frac{g}{4},\ g_{K^*\Lambda\Xi}=\frac{\sqrt{3}}{4}g,\ g_{K^*\Sigma\Xi}=\frac{g}{4},\\
&\frac{f_{\pi\Lambda\Sigma}}{m_\pi}=\frac{1}{\sqrt{3}}g',\ \frac{f_{\pi\Sigma\Sigma}}{m_\pi}=-\alpha g',\ \frac{f_{\pi\Xi\Xi}}{m_\pi}=\frac{1-\alpha}{2}g',\\
&\frac{f_{\eta\Lambda\Lambda}}{m_\eta}=-\left(\frac{\cos\theta}{\sqrt{3}}+\sqrt{\frac{2}{3}}\sin\theta\right)g',\\
&\frac{f_{\eta\Sigma\Sigma}}{m_\eta}=\left(\frac{\cos\theta}{\sqrt{3}}-\sqrt{\frac{2}{3}}\sin\theta\right)g',\\
&\frac{f_{\eta\Xi\Xi}}{m_\eta}=-\left(\frac{3\alpha+1}{2\sqrt{3}}\cos\theta+\sqrt{\frac{2}{3}}\sin\theta\right)g',\\
&\frac{f_{KN\Lambda}}{m_K}=-\frac{3\alpha+1}{2\sqrt{3}}g',\ \frac{f_{KN\Sigma}}{m_K}=\frac{1-\alpha}{2}g',\\
&\frac{f_{K\Lambda\Xi}}{m_K}=\frac{3\alpha-1}{2\sqrt{3}}g',\ \frac{f_{K\Sigma\Xi}}{m_K}=\frac{1+\alpha}{2}g'.
\end{aligned}\tag{8}$$

The above hadronic coupling constants can be related to the coupling constants between pion and rho meson with nucleon, which are defined by

$$\begin{aligned}
\mathcal{L}_{\pi NN}&=\frac{f_{\pi NN}}{m_\pi}\bar{N}\gamma^5\gamma^\mu\vec{\tau}N\cdot\partial_\mu\vec{\pi},\\
\mathcal{L}_{\rho NN}&=g_{\rho NN}\bar{N}\gamma^\mu\vec{\tau}N\cdot\vec{\rho}_\mu,
\end{aligned}\tag{9}$$

with

$$\frac{f_{\pi NN}}{m_\pi}=\frac{1+\alpha}{2}g',\quad g_{\rho NN}=\frac{g}{4}.\tag{10}$$

From the empirical values $f_{\pi NN}=1.00$, $g_{\rho NN}=3.25$ [14], and $D/(D+F)=1/(1+\alpha)=0.64$ [15], we obtain $g'=9.2$ GeV^{-1}, $g=13.0$, and $\alpha=0.56$. Substituting these parameters into Eq. (8) gives us the hadronic coupling constants in the interaction Lagrangians. Their values are given in Table I.

Vertex	f	Vertex	g	Vertex	g	g^t
πNN	1.00	$\rho\pi\pi$	3.25	ρNN	3.25	19.8
$\pi\Lambda\Sigma$	0.741	ρKK	-3.25	$\rho\Lambda\Sigma$	0.0	17.9
$\pi\Sigma\Sigma$	-0.722	ωKK	-3.25	$\rho\Sigma\Sigma$	-6.50	-18.0
$\pi\Xi\Xi$	0.281	ϕKK	4.60	$\rho\Xi\Xi$	-3.25	7.79
$\eta\Lambda\Lambda$	-1.06	$K^*K\pi$	3.25	$\omega\Lambda\Lambda$	0.0	10.0
$\eta\Sigma\Sigma$	4.26	$K^*K\eta$	5.18	$\omega\Sigma\Sigma$	0.0	32.1
$\eta\Xi\Xi$	-1.98			$\phi\Lambda\Lambda$	0.0	28.4
$KN\Lambda$	-3.52			$K^*\Lambda\Xi$	5.63	6.52
$KN\Sigma$	0.992			$K^*\Sigma\Xi$	3.25	26.4
$K\Lambda\Xi$	0.900					
$K\Sigma\Xi$	3.54					

TABLE I: Coupling constants used in the present study. They are determined from empirically known coupling constants using relations derived from the SU(3) symmetry.

C. Tensor interactions

Besides the vector interactions between vector mesons and baryons introduced in Eq.(4) through the minimal substitution, there also exist tensor interactions. In the present study, we assume that the tensor interactions are SU(3) invariant and have both D and F type as the interactions between pseudoscalar mesons and baryons. The vector meson and baryon interaction Lagrangian can then be written as

$$\begin{aligned}
\mathcal{L}_{VBB}=&\ g\mathrm{Tr}(\bar{B}\gamma^\mu V_\mu B)+\frac{g^t}{2m}\mathrm{Tr}\left[(1-\alpha)\bar{B}\sigma^{\mu\nu}B\partial_\mu V_\nu\right.\\
&+\left.(1+\alpha)(\partial_\mu V_\nu)\bar{B}\sigma^{\mu\nu}B\right],
\end{aligned}\tag{11}$$

where m is the SU(3) degenerate baryon mass and g^t is the universal tensor coupling constant. To include the symmetry breaking effect, we replace $2m$ in the above equation by the average empirical masses of the two baryons at an interaction vertex. One usually introduces the parameter $\kappa=g^t/g$ to denote the ratio of tensor to vector couplings.

Expanding Eq.(11) using the matrix representations of the vector mesons and baryons, we obtain the following relations among tensor coupling constants

$$\begin{aligned}
\frac{g^t_{\rho\Lambda\Sigma}}{m_\Lambda+m_\Sigma}&=\frac{2}{\sqrt{3}(1+\alpha)}\frac{g^t_{\rho NN}}{2m_N},\\
\frac{g^t_{\rho\Sigma\Sigma}}{2m_\Sigma}&=-\frac{2\alpha}{1+\alpha}\frac{g^t_{\rho NN}}{2m_N},\\
\frac{g^t_{\rho\Xi\Xi}}{2m_\Xi}&=\frac{1-\alpha}{1+\alpha}\frac{g^t_{\rho NN}}{2m_N},\\
\frac{g^t_{\omega\Lambda\Lambda}}{2m_\Lambda}&=\frac{2}{3(1+\alpha)}\frac{g^t_{\rho NN}}{2m_N},\\
\frac{g^t_{\omega\Sigma\Sigma}}{2m_\Sigma}&=\frac{2}{1+\alpha}\frac{g^t_{\rho NN}}{2m_N},
\end{aligned}$$

$$
\begin{aligned}
\frac{g^t_{\phi\Lambda\Lambda}}{2m_\Lambda} &= \frac{4\sqrt{2}}{3(1+\alpha)}\frac{g^t_{\rho NN}}{2m_N},\\
\frac{g^t_{K^*\Lambda\Xi}}{m_\Lambda+m_\Xi} &= \frac{3\alpha-1}{\sqrt{3}(1+\alpha)}\frac{g^t_{\rho NN}}{2m_N},\\
\frac{g^t_{K^*\Sigma\Xi}}{m_\Xi+m_\Sigma} &= \frac{g^t_{\rho NN}}{2m_N}.
\end{aligned} \tag{12}
$$

From the empirical value for the rho meson tensor interaction with nucleons, i.e., $g^t_{\rho NN} = 19.8$ [14], we obtain from Eq.(12) the tensor coupling constants shown in Table I.

III. THE COUPLED-CHANNEL APPROACH

In Refs. [9,10], a coupled-channel approach based on a Lagrangian similar to the one introduced in Section II has been used for evaluating the cross sections for the strangeness-exchange reactions $\bar{K}N \to \pi\Lambda$ and $\bar{K}N \to \pi\Sigma$. In this paper, we extend the couple-channel method to study the reactions $\bar{K}\Lambda \to \pi\Xi$ and $\bar{K}\Sigma \to \pi\Xi$ for Ξ production. We further consider reactions involving an eta meson instead of a pion in the final state.

The transition matrix in the present study is a 4 × 4 matrix with matrix elements denoting the transition amplitudes between the four channels $\bar{K}\Lambda$, $\bar{K}\Sigma$, $\pi\Xi$, and $\eta\Xi$. In the coupled-channel approach, the transition matrix satisfies the Bethe-Salpeter equation,

$$T = V + VGT. \tag{13}$$

In the above, V is the transition potential consisting of all one- and two-particle irreducible connected diagrams, and G is the dressed propagator.

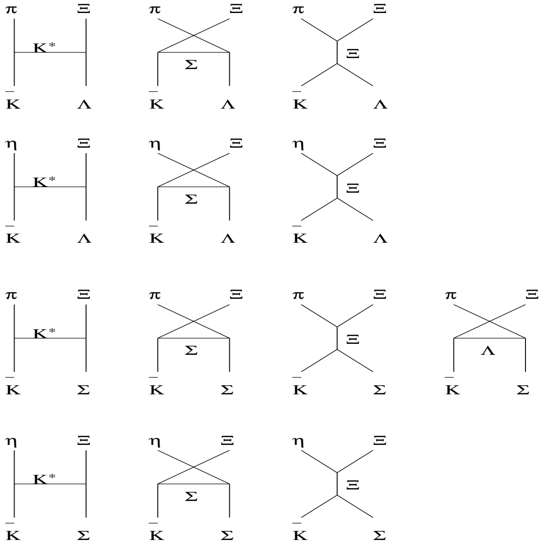

FIG. 1. Born diagrams for Ξ production from strangeness exchange reactions.

Following Refs. [9,10], we include in the transition potential V only the lowest-order Born diagrams. The diagrams in Fig. 1 are for the strangeness-exchange reactions leading to Ξ production. Figs. 2 and 3 give, respectively, the diagrams for the elastic and inelastic meson-baryon scattering processes.

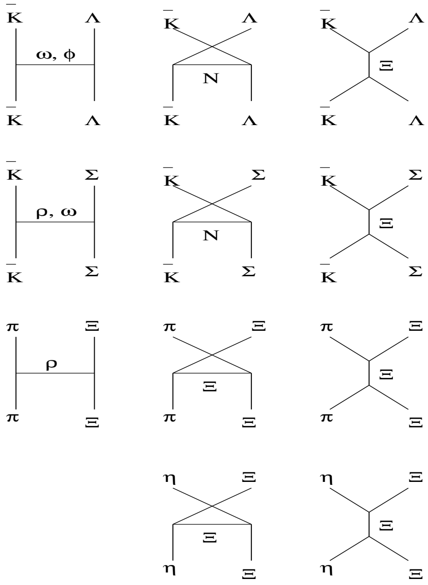

FIG. 2. Elastic scattering between mesons and hyperons.

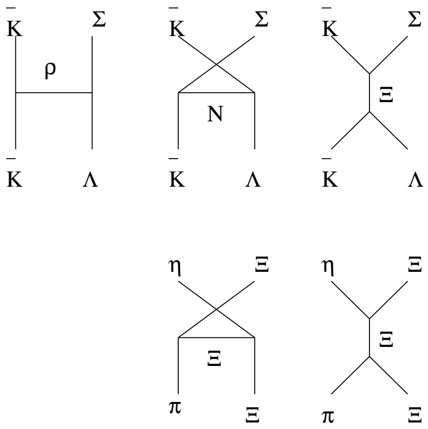

FIG. 3. Inelastic scattering between mesons and hyperons.

The Bethe-Salpeter equation can be rewritten in terms of the imaginary part of the propagator, $G_{\rm I}$, as

$$T = K + KG_{\rm I}T, \tag{14}$$

where the K matrix satisfies the equation

$$K = V + VG_{\rm R}K, \tag{15}$$

with $G_{\rm R}$ denoting the real part of the propagator.

Following the frequently used K-matrix approximation, we set $K = V$, i.e., neglecting the real part of G or the off-shell contribution in the intermediate states. As shown in Ref. [10], using the on-shell propagator

$$\begin{aligned} G_{\mathrm{I}} &= -2i\pi^2\delta(k_m^2 - m_m^2)\delta(k_b^2 - m_b^2) \\ &\quad \times \theta(k_m^0)\theta(k_b^0)(\not{k}_b + m_b), \end{aligned} \tag{16}$$

with m_m and m_b the masses of intermediate meson and baryon, respectively, leads to a simple relation between the transition matrix T and the transition potential V, i.e.,

$$T = \frac{V}{1 + iV}. \tag{17}$$

It can be shown that the K-matrix approximation preserves the unitarity of the transition matrix [10]. However, because of the neglect of G_{R}, the scattering amplitude obtained from the K-matrix approximation may not have the full analytic structure of the exact scattering amplitude. On the other hand, it has been shown in Ref. [16] that for pion-nucleon scattering the results from the Bethe-Salpeter equation are not very sensitive to the approximation used for the propagator.

IV. CALCULATION DETAILS

A. Born amplitudes

Using the interaction Lagrangians in Section II, the amplitudes for the Born diagrams shown in Figs. 1, 2, and 3 can be straightforwardly derived. Aside from isospins, they are given generically by

$$\begin{aligned} M_t &= g_1\ (q_{i\mu} + q_{f\mu})\frac{g^{\mu\nu} - q_t^\mu q_t^\nu/m_t^2}{t - m_t^2} \\ &\quad \times \bar{u}_f\left[(g_2 + g^t)\gamma_\nu - g^t\frac{p_{i\nu} + p_{f\nu}}{M_i + M_f}\right]u_i, \end{aligned} \tag{18}$$

$$\begin{aligned} M_u &= \frac{f_i}{m_i}\frac{f_f}{m_f}\frac{1}{u - m_u^2}\bar{u}_f\not{q}_i(m_u - \not{q}_u)\not{q}_f u_i, \\ M_s &= \frac{f_i}{m_i}\frac{f_f}{m_f}\frac{1}{s - m_s^2}\bar{u}_f\not{q}_i(m_s - \not{q}_s)\not{q}_f u_i, \end{aligned} \tag{19}$$

for the t, u and s channels, respectively. In the above, q_i and q_f are the momenta of the initial and final mesons with masses m_i and m_f, respectively; u_i is the Dirac spinor for the initial baryon with mass M_i and momentum p_i, while u_f is that for the final baryon with mass M_f and momentum p_f; and q_t, q_u and q_s are the momenta of the intermediate particles with masses m_t, m_u and m_s in the three channels. The coupling constants g_1 and g_2 in the t channel amplitude denote, respectively, the coupling of the exchanged vector meson with pseudoscalar mesons and baryons. The couplings of the initial and final mesons with baryons in the u and s channel are given by f_i and f_f, respectively. Explicit expressions including isospins for the amplitudes of all diagrams in Figs. 1, 2, and 3 are given in Appendix A.

Because of the finite size of hadrons, form factors are needed at interaction vertices. All form factors are taken to have the form

$$F(\mathbf{q}^2) = \frac{\Lambda^2}{\Lambda^2 + \mathbf{q}^2}. \tag{20}$$

In the above, the momentum $\mathbf{q}$ is the three momentum transfer for t channel diagrams, and the center-of-mass momentum of the initial and finial mesons for u and s channel diagrams. The cutoff parameter Λ is a parameter and will be varied in our study. To reduce the number of free parameters, we use the same cutoff parameter for all vertices.

B. partial wave expansion

For processes involving pseudoscalar mesons and spin-half baryons as studied here, the orbital angular momentum is the same for the initial and the final state. As shown in Ref. [10], the relation given in Eq. (17) between the transition amplitude and the transition potential obtained in the K-matrix approximation also applies to the transition matrix for a given total angular momentum j and orbital angular momentum l, i.e.,

$$T'_{jl} = \frac{V'_{jl}}{1 + iV'_{jl}}, \tag{21}$$

where T' and V' are related to T and V by

$$\begin{aligned} T(p_i, p_f) &= \frac{4\pi}{\sqrt{\mathrm{p_i p_f}}}T'(p_i, p_f), \\ V(p_i, p_f) &= \frac{4\pi}{\sqrt{\mathrm{p_i p_f}}}V'(p_i, p_f), \end{aligned} \tag{22}$$

with $\mathrm{p_i}$ and $\mathrm{p_f}$ the magnitude of initial and final baryon three momenta in the center-of-mass frame.

The total cross section is then given by

$$\sigma_{\mathrm{total}} = \frac{1}{4\pi}\frac{\mathrm{p_f}}{\mathrm{p_i}}\sum_l\left[lT_{l-}^2 + (l+1)T_{l+}^2\right], \tag{23}$$

where $T_{l\pm}$ denotes $T_{l\pm\frac{1}{2},l}$.

To derive V_{jl} from the the Born amplitudes, we use the following relations given in Refs. [17,18]:

$$\frac{V_{l\pm}}{4\pi} = \frac{1}{2}\int_{-1}^{1}(\tilde{A}P_l + \tilde{B}P_{l\pm1})dx, \tag{24}$$

where $V_{l\pm} = V_{l\pm\frac{1}{2},l}$ and

$$\tilde{A} = \frac{\sqrt{(E_i + M_i)(E_f + M_f)}}{8\pi\sqrt{s}}[A + B(\sqrt{s} - \bar{M})], \tag{25}$$

$$\tilde{B} = \frac{\sqrt{(E_i - M_i)(E_f - M_f)}}{8\pi\sqrt{s}}[-A + B(\sqrt{s} + \bar{M})]. \tag{26}$$

In the above, $\bar{M} = (M_i + M_f)/2$ is the average of the initial and final baryon masses; and E_i and E_f are, respectively, the initial and final baryon energies.

The spin-independent (A) and spin-dependent (B) amplitudes are defined by

$$M_{fi} = \bar{u}(p_f, s_f)\left[A + \frac{B}{2}(\not{q}_i + \not{q}_f)\right]u(p_i, s_i), \tag{27}$$

and can be evaluated according to

$$\begin{aligned} A &= A_s + A_t + A_u, \\ B &= B_s + B_t + B_u. \end{aligned} \tag{28}$$

The various terms on the right-hand side of the above equation are obtained from the Born amplitudes, and aside from isospins they are given explicitly by

$$\begin{aligned} A_s &= \frac{f_i}{m_i}\frac{f_f}{m_f}\frac{1}{s - m_s^2}\left\{m_s\left[s - \frac{1}{2}(M_i^2 + M_f^2)\right]\right. \\ &\quad \left. - \frac{1}{2}(M_i + M_f)(M_i M_f - s)\right\}, \end{aligned} \tag{29}$$

$$\begin{aligned} B_s &= \frac{f_i}{m_i}\frac{f_f}{m_f}\frac{1}{s - m_s^2}[-m_u(M_i + M_f) \\ &\quad - s - m_i m_f], \end{aligned} \tag{30}$$

for the s channel Born amplitude,

$$\begin{aligned} A_t &= \frac{g_1}{t - m_t^2}\left[\frac{g_2}{m_t^2}(m_i^2 - m_f^2)(M_i - M_f)\right. \\ &\quad \left. - \frac{g^t}{M_i + M_f}(q_i + q_f)\cdot(p_i + p_f)\right], \end{aligned} \tag{31}$$

$$B_t = \frac{2g_1(g_2 + g^t)}{t - m_t^2}, \tag{32}$$

for the t channel Born amplitude, and

$$\begin{aligned} A_u &= \frac{f_i}{m_i}\frac{f_f}{m_f}\frac{1}{u - m_u^2}\left\{(m_u + M_f)\left[s - 2E_f E_i\sqrt{s}\right.\right. \\ &\quad \left. + 2p_f\cdot p_i - M_i M_f + \frac{1}{2}(M_i + M_f)^2\right] \\ &\quad \left. - \frac{1}{2}(2q_i\cdot p_f - m_i^2)(M_i - M_f)\right\}, \end{aligned} \tag{33}$$

$$\begin{aligned} B_u &= \frac{f_i}{m_i}\frac{f_f}{m_f}\frac{1}{u - m_u^2}[(m_u + M_f)(M_i + M_f) \\ &\quad + m_i^2 - 2q_i\cdot p_f], \end{aligned} \tag{34}$$

for the u channel Born amplitude.

V. RESULTS

In this section, we show both the total and differential cross sections obtained from the coupled-channel approach for the strangeness-exchange reactions $\bar{K}\Lambda \to \pi\Xi$, $\bar{K}\Sigma \to \pi\Xi$, $\bar{K}\Lambda \to \eta\Xi$, and $\bar{K}\Sigma \to \eta\Xi$. These results will be compared with those obtained from the Born approximation. We further show the total cross sections for the elastic processes $\bar{K}\Lambda \to \bar{K}\Lambda$, $\bar{K}\Sigma \to \bar{K}\Sigma$, $\pi\Xi \to \pi\Xi$, and $\eta\Xi \to \eta\Xi$ as well as for the inelastic processes $\bar{K}\Lambda \to \bar{K}\Sigma$ and $\pi\Xi \to \eta\Xi$. All cross sections are obtained from Eq.(23) by averaging over initial and summing over final particle spins and isospins.

A. Strangeness-exchange reactions

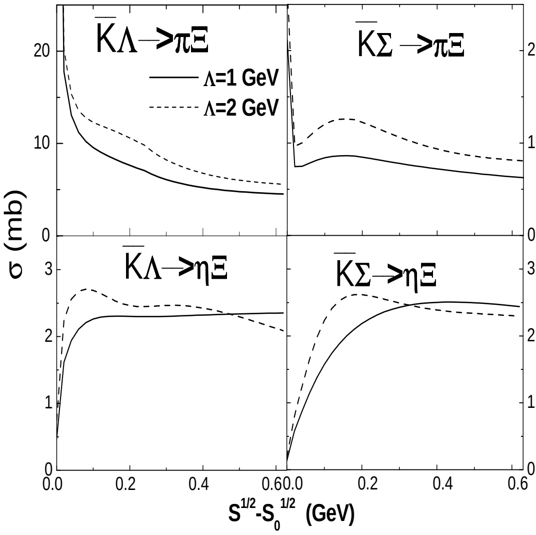

FIG. 4. Cross sections for Ξ production in strangeness exchange reactions as functions of center-of-mass energy from the coupled-channel approach with cutoff parameters $\Lambda = 1$ (solid curves) and 2 GeV (dotted curves).

Results on the cross sections for Ξ production from the strangeness-exchange reactions $\bar{K}\Lambda \to \pi\Xi$, $\bar{K}\Sigma \to \pi\Xi$, $\bar{K}\Lambda \to \eta\Xi$, and $\bar{K}\Sigma \to \eta\Xi$ are shown in Fig. 4. These cross sections are evaluated using the coupled-channel approach with cutoff parameters $\Lambda = 1$ and 2 GeV. It is seen that the cross sections do not depend strongly on the value of the cutoff parameter. Since the reactions with pions in the final state is exothermic, their cross sections diverge at threshold. On the other hand, the reactions with etas in the final state are endothermic and have thus vanishing cross section at threshold. For all four reactions, the cross sections at energies much above threshold are a few mb, with those involving pions in the final state about twice as large as those involving etas in the final state.

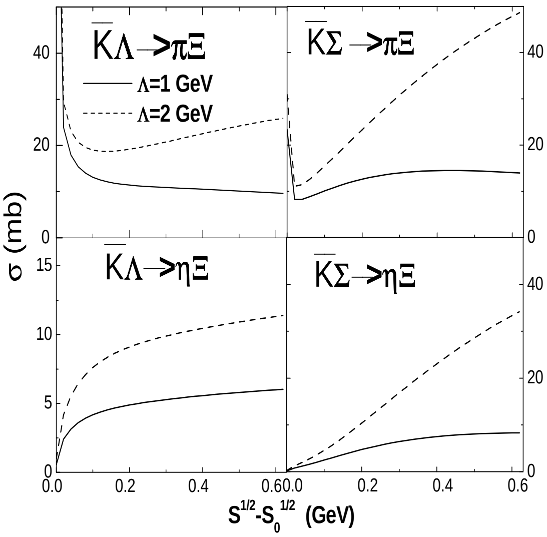

FIG. 5. Cross sections for Ξ production in strangeness exchange reactions as functions of center-of-mass energy from the Born approximation with cutoff parameters $\Lambda = 1$ (solid curves) and 2 GeV (dotted curves).

The results from the coupled-channel approach are very different from those given by the Born approximation. As shown in Fig. 5, the cross sections evaluated using the Born approximation have a stronger dependence on the value of the cutoff parameter than those from the coupled-channel approach. Furthermore, cross sections from the Born approximation in general increase with center-of-mass energy much faster than those from the coupled-channel approach, particularly for the processes $\bar{K}\Sigma \to \pi\Xi$ and $\bar{K}\Sigma \to \eta\Xi$. As a result, the Born approximation gives a much larger cross section than the corresponding one from the coupled-channel approach. The difference is large for the larger cutoff parameter. This is easily seen from Eq.(17), as the transition amplitude from the coupled-channel approach is bounded as the magnitude of the transition potential increases. Our results thus demonstrate the importance of the unitarity constraint, which is satisfied in the coupled-channel approach, on the determination of the magnitude for the Ξ production cross sections.

We have also evaluated the differential cross sections for the strangeness-exchange reactions, and the results at center-of-mass energies of 0.05, 0.1, 0.2, and 0.3 GeV above the threshold are shown in Fig.6. As expected, the angular distribution is relatively flat near threshold and becomes more forward peaked as the energy increases. For all four processes, the shapes of their differential cross sections from the coupled-channel approach are, however, similar to those obtained from the Born approximation, which are shown in Fig. 7.

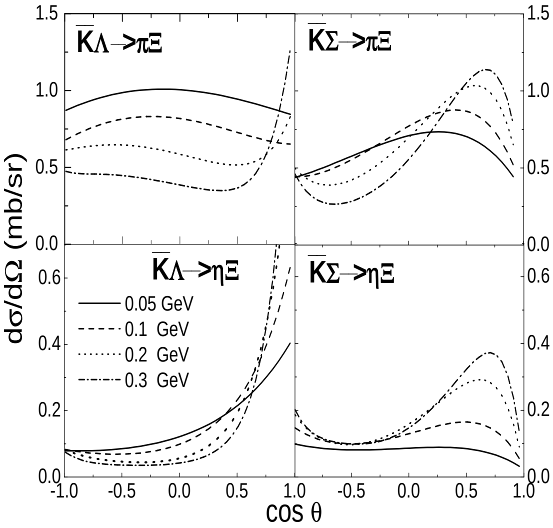

FIG. 6. Differential cross sections for strangeness-exchange reactions obtained from the coupled-channel approach at different center-of-mass energies above the threshold.

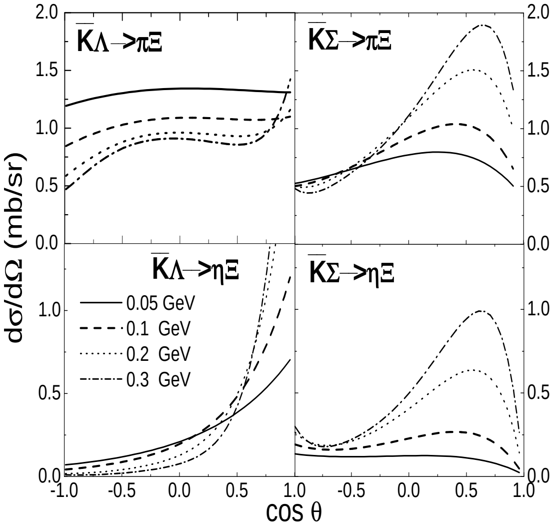

FIG. 7. Differential cross sections for strangeness-exchange reactions obtained from the Born approximation at different center-of-mass energies above the threshold.

B. Elastic and inelastic scattering processes

The transition matrix T also contains information on the cross sections for the elastic processes $\bar{K}\Lambda \to \bar{K}\Lambda$, $\bar{K}\Sigma \to \bar{K}\Sigma$, $\pi\Xi \to \pi\Xi$, and $\eta\Xi \to \eta\Xi$ as well as for the inelastic processes $\bar{K}\Lambda \to \bar{K}\Sigma$ and $\pi\Xi \to \eta\Xi$. The results are shown in Fig. 8. As in the case of strangeness-exchange reactions, these cross sections do not depend strongly on the cutoff parameter. All four elastic scattering cross sections are relatively large. For inelastic processes, the cross section for $\bar{K}\Lambda \to \bar{K}\Sigma$ is a few mb but it is less than one mb for the reaction $\pi\Xi \to \eta\Xi$.

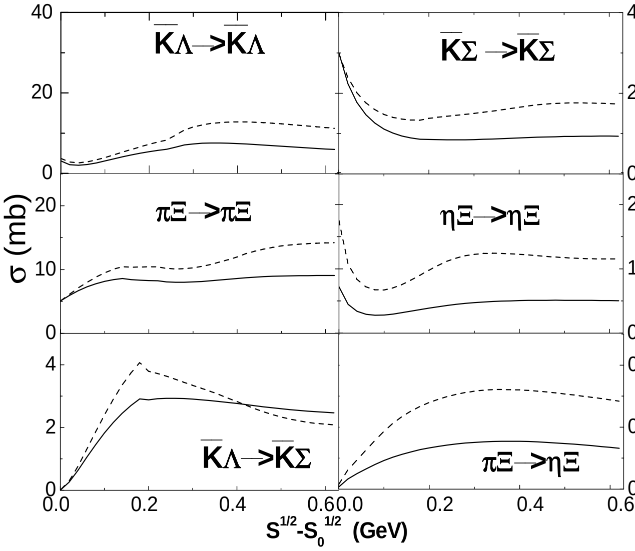

FIG. 8. Cross sections for elastic and inelastic processes from the coupled-channel approach for cutoff parameters $\Lambda = 1$ GeV (solid curves) and $\Lambda = 2$ GeV (dash curves).

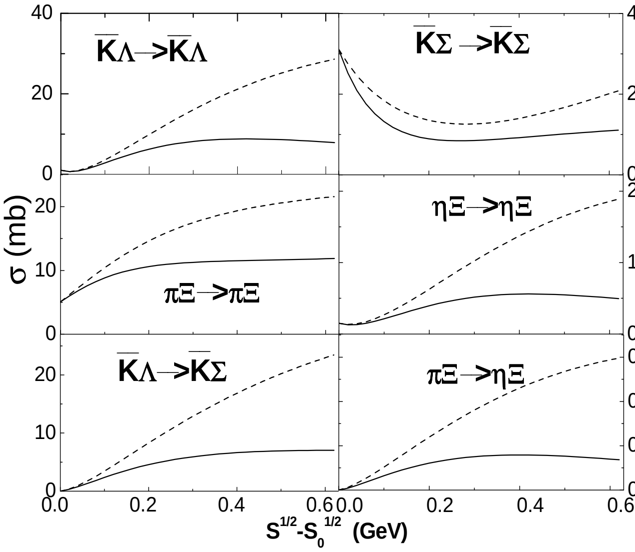

FIG. 9. Cross sections for elastic and inelastic processes obtained from the Born approximation with cutoff parameters $\Lambda = 1$ GeV (solid curves) and $\Lambda = 2$ GeV (dash curves).

For comparisons, we show in Fig. 9 the cross sections for the elastic and inelastic processes obtained from the Born approximation. It is seen that the results depend strongly on the value of the cutoff parameter. Except for the reaction $\eta\Xi \to \eta\Xi$, the Born approximation gives much larger cross sections than the coupled-channel approach if the cutoff parameter is $\Lambda = 2$ GeV. However, with a smaller cutoff parameter of $\Lambda = 1$ GeV, the results from the two approaches become comparable. The cross section for the reaction $\eta\Xi \to \eta\Xi$ in the Born approximation is much smaller than that for the reaction $\pi\Xi \to \pi\Xi$ due to the absence of t channel diagram as shown in Fig. 2. Comparing the Born cross section for the reaction $\eta\Xi \to \eta\Xi$ with that from the coupled-channel approach shows that the coupled-channel effect increases its cross section significantly.

Another difference between the cross sections from the coupled-channel approach and those from the Born approximation is that the former do not have as smooth an energy dependence as the latter. This is due to the fact that in the coupled-channel approach the coupling to a different channel in the intermediate states is enhanced whenever the energy is above its threshold. For example, in the reaction $\pi\Xi \to \pi\Xi$, which has the lowest total channel mass, effects of other channels such as $\bar{K}\Lambda$, $\bar{K}\Sigma$, and $\eta\Xi$ appears successively with increasing energy as shown in Fig. 8.

C. Mixing angle dependence

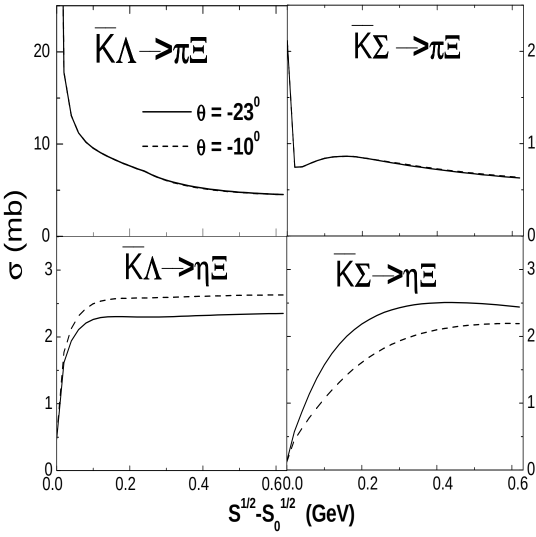

FIG. 10. Cross sections for strangeness-exchange reactions using two different mixing angles between the singlet and octet eta mesons. The cut-off parameter is $\Lambda = 1$ GeV in both cases.

To see the dependence of our results on the mixing angle between the singlet and octet eta mesons, we have also calculated the cross sections for the strangeness-exchange reactions using a mixing angle of $\theta = -10^\circ$ and a cutoff parameter of $\Lambda = 1$ GeV. In Fig. 10, we compare the results with those using $\theta = -23^\circ$ and the same cutoff parameter. We find that the cross sections for the reactions $\bar{K}\Lambda \to \pi\Xi$ and $\bar{K}\Sigma \to \pi\Xi$ are essentially the same for the two mixing angles as the eta meson affects their cross sections only indirectly through the coupled-channel effect. For the reactions $\bar{K}\Lambda \to \eta\Xi$ and $\bar{K}\Sigma \to \eta\Xi$ involving the eta meson in the final state, there are slightly variations between the cross sections from the two mixing angles.

VI. CONCLUSIONS

To evaluate the Ξ production cross section from the strangeness-exchange reactions between $\bar{K}$ and hyperons Λ and Σ, we have carried out a coupled-channel calculation including the four channels $\bar{K}\Lambda$, $\bar{K}\Sigma$, $\pi\Xi$, and $\eta\Xi$. The resulting coupled-channel Bethe-Salpeter equation for the transition matrix is solved in the K-matrix approximation, i.e., neglecting the real part of the propagator or the off-shell contribution in the Bethe-Salpeter equation.

The transition potential, which drives the higher-order effects in the Bethe-Salpeter equation, is obtained from the lowest-order Born diagrams for processes between these channels. The Born diagrams, which generally include the s, t, and u channels, are evaluated from a gauged SU(3) flavor invariant Lagrangian. The symmetry breaking effect is taken into account by using empirical masses. For coupling constants in the interaction Lagrangians, they are determined from empirically known coupling constants using relations derived from the SU(3) symmetry. Form factors are then introduced at interaction vertices to take into account the finite size of hadrons.

Both total and differential cross sections for the strangeness-exchange reactions $\bar{K}\Lambda \to \pi\Xi$, $\bar{K}\Sigma \to \pi\Xi$, $\bar{K}\Lambda \to \eta\Xi$, and $\bar{K}\Sigma \to \eta\Xi$ are evaluated. We find that values of these cross sections are not small and are not very dependent on the values of the cutoff parameters introduced in the form factors. This is in contrast with the cross sections evaluated in the Born approximation, which shows a much stronger dependence on the cutoff parameter. Our results thus demonstrate the importance of unitarity, which is satisfied by the coupled-channel approach in the K-matrix approximation but not in the Born approximation, in evaluating the cross section for Ξ production from strangeness-exchange reactions.

As a byproduct of our study, we have also obtained the cross sections for the elastic process $\bar{K}\Lambda \to \bar{K}\Lambda$, $\bar{K}\Sigma \to \bar{K}\Sigma$, $\pi\Xi \to \pi\Xi$, and $\eta\Xi \to \eta\Xi$ as well as for the inelastic processes $\bar{K}\Lambda \to \bar{K}\Sigma$ and $\pi\Xi \to \eta\Xi$. As for the strangeness-exchange reactions, the cross sections obtained from the coupled-channel approach are less dependent on the cutoff parameters than those from the Born approximation.

The results from our study are useful for relativistic heavy ion collisions. Values of the Ξ production cross sections from our study are not small and are comparable to those used in a recent transport model calculations [3]. In this study, it has been found that the strangeness-exchange reactions play an important role in the production of multistrange baryons such as Ξ and Ω in heavy ion collisions at the SPS energies if one does not assume that the quark-gluon plasma is formed in the collisions.

Heavy ion collisions at energies below the production threshold for Ξ in the nucleon-nucleon interaction may be useful for testing the results obtained in present study. If the heavy ion collision energy is above the thresholds for $\bar{K}$, Λ and Σ, which are lower than that for Ξ, Ξ can still be produced via the $\bar{K}$ induced strangeness-exchange reactions on Λ and Σ. The Ξ yield in heavy ion collisions at such subthreshold energies is thus sensitive to the cross sections for these strangeness-exchange reactions. A similar idea via the strangeness-exchange reaction $\pi\Lambda \to \bar{K}N$ [19–21] has been found to be important for explaining the observed enhancement of K^- production in heavy ion collisions at energies below its production threshold in the nucleon-nucleon interaction [22].

For future studies, it would be of interest to extend present study to Ω production from the strangeness-exchange reactions $\bar{K}\Xi \to \pi\Omega$ and $\bar{K}\Xi \to \eta\Omega$. This is particular important as the enhancement of Ω production in relativistic heavy ion collisions is even larger than that for Ξ [23]. Knowledge of these cross sections is thus needed to determine if these strangeness-exchange reactions also contribute significantly to Ω production in relativistic heavy ion collisions. Since Ω belongs to the decuplet representation of SU(3), both the interaction Lagrangians and the partial wave expansion involved in the calculation will be different from those for Ξ, which belongs to the octet representation of SU(3).

It will also be of interest to improve the results from the coupled-channel approach by including the off-shell effects due to the real part of the propagator in the Bethe-Salpeter equation, which has been neglected in the present study.

Finally, there also exists other approach to the reactions $\bar{K}N \to \pi\Lambda$ and $\bar{K}N \to \pi\Sigma$ based on the $SU(3) \times SU(3)$ chiral Lagrangian [24]. Since chiral symmetry imposes additional constrains on meson-baryon scattering amplitudes at low-energies, it is important to see how the results obtained from present approach are modified by chiral symmetry.

ACKNOWLEDGMENTS

We are grateful to Zi-wei Lin and Wei Liu for helpful discussions. This paper is based on work supported by the National Science Foundation under Grant Nos. PHY-9870038 and PHY-0098805, the Welch Foundation under

Grant No. A-1358, and the Texas Advanced Research Program under Grant No. FY99-010366-0081.

APPENDIX

In this appendix, we give explicit expressions for the amplitudes of all the diagrams in Figs. 1, 2, and 3.

1) $\bar{K}\Lambda \to \pi\Xi$:

$$\begin{aligned} M_t &= g_{K^*K\pi} g_{K^*\Lambda\Xi}\ \tau^a_{ij}\ (p_{K_i\mu} + p_{\pi^a\mu}) \\ &\quad \times \frac{g^{\mu\nu} - q_t^\mu q_t^\nu / m^2_{K^*}}{t - m^2_{K^*}} \\ &\quad \times \bar{\Xi}_j \left[(1+\kappa)\gamma_\nu - \kappa \frac{p_{\Lambda\nu} + p_{\Xi_\nu}}{m_\Lambda + m_\Xi} \right] \Lambda, \end{aligned} \tag{1}$$

$$\begin{aligned} M_u &= \frac{f_{K\Sigma\Xi}}{m_K} \frac{f_{\pi\Sigma\Lambda}}{m_\pi}\ \tau^a_{ij}\ \frac{1}{u - m^2_\Sigma} \\ &\quad \times \bar{\Xi}_j \not{p}_{K_i} (m_\Sigma - \not{q}_u) \not{p}_{\pi^a} \Lambda, \end{aligned} \tag{2}$$

$$\begin{aligned} M_s &= \frac{f_{K\Lambda\Xi}}{m_K} \frac{f_{\pi\Xi\Xi}}{m_\pi}\ \tau^a_{ij}\ \frac{1}{s - m^2_\Xi} \\ &\quad \times \bar{\Xi}_j \not{p}_{\pi^a} (m_\Xi - \not{q}_s) \not{p}_{K_i} \Lambda. \end{aligned} \tag{3}$$

2) $\bar{K}\Lambda \to \eta\Xi$:

$$\begin{aligned} M_t &= g_{K^*K\eta} g_{K^*\Lambda\Xi}\ \delta_{ij}\ (p_{K_i\mu} + p_{\eta\mu}) \\ &\quad \times \frac{g^{\mu\nu} - q_t^\mu q_t^\nu / m^2_{K^*}}{t - m^2_{K^*}} \\ &\quad \times \bar{\Xi}_j \left[(1+\kappa)\gamma_\nu - \kappa \frac{p_{\Lambda\nu} + p_{\Xi_\nu}}{m_\Lambda + m_\Xi} \right] \Lambda, \end{aligned} \tag{4}$$

$$\begin{aligned} M_u &= \frac{f_{K\Sigma\Xi}}{m_K} \frac{f_{\eta\Sigma\Lambda}}{m_\eta}\ \delta_{ij}\ \frac{1}{u - m^2_\Lambda} \\ &\quad \times \bar{\Xi}_j \not{p}_{K_i} (m_\Lambda - \not{q}_u) \not{p}_{\eta} \Lambda, \end{aligned} \tag{5}$$

$$\begin{aligned} M_s &= \frac{f_{K\Lambda\Xi}}{m_K} \frac{f_{\eta\Xi\Xi}}{m_\eta}\ \delta_{ij}\ \frac{1}{s - m^2_\Xi} \\ &\quad \times \bar{\Xi}_j \not{p}_{\eta} (m_\Xi - \not{q}_s) \not{p}_{K_i} \Lambda. \end{aligned} \tag{6}$$

3) $\bar{K}\Sigma \to \pi\Xi$:

$$\begin{aligned} M_t &= g_{K^*K\pi} g_{K^*\Sigma\Xi}\ (\tau^a\tau^b)_{ij}\ (p_{K_i\mu} + p_{\pi^a\mu}) \\ &\quad \times \frac{g^{\mu\nu} - q_t^\mu q_t^\nu / m^2_{K^*}}{t - m^2_{K^*}} \\ &\quad \times \bar{\Xi}_j \left[(1+\kappa)\gamma_\nu - \kappa \frac{p_{\Sigma\nu} + p_{\Xi_\nu}}{m_\Sigma + m_\Xi} \right] \Sigma^b, \end{aligned} \tag{7}$$

$$\begin{aligned} M_{u1} &= \frac{f_{K\Sigma\Xi}}{m_K} \frac{f_{\pi\Sigma\Sigma}}{m_\pi}\ i\epsilon^{dba}\tau^d_{ij}\ \frac{1}{u - m^2_\Sigma} \\ &\quad \times \bar{\Xi}_j \not{p}_{K_i} (m_\Sigma - \not{q}_u) \not{p}_{\pi^a} \Sigma^b, \end{aligned} \tag{8}$$

$$\begin{aligned} M_{u2} &= \frac{f_{K\Lambda\Xi}}{m_K} \frac{f_{\pi\Sigma\Lambda}}{m_\pi}\ \delta_{ab}\delta_{ij}\ \frac{1}{u - m^2_\Lambda} \\ &\quad \times \bar{\Xi}_j \not{p}_{K_i} (m_\Lambda - \not{q}_u) \not{p}_{\pi^a} \Sigma^b, \\ M_s &= \frac{f_{K\Sigma\Xi}}{m_K} \frac{f_{\pi\Xi\Xi}}{m_\pi}\ (\tau^b\tau^a)_{ij}\ \frac{1}{s - m^2_\Xi} \\ &\quad \times \bar{\Xi}_j \not{p}_{\pi^a} (m_\Xi - \not{q}_s) \not{p}_{K_i} \Sigma^b. \end{aligned} \tag{9}$$

4) $\bar{K}\Sigma \to \eta\Xi$:

$$\begin{aligned} M_t &= g_{K^*K\eta} g_{K^*\Sigma\Xi}\ \tau^a_{ij}\ (p_{K\mu} + p_{\eta\mu}) \\ &\quad \times \frac{g^{\mu\nu} - q_t^\mu q_t^\nu / m^2_{K^*}}{t - m^2_{K^*}} \\ &\quad \times \bar{\Xi}_j \left[(1+\kappa)\gamma_\nu - \kappa \frac{p_{\Sigma\nu} + p_{\Xi_\nu}}{m_\Sigma + m_\Xi} \right] \Sigma^a, \end{aligned} \tag{10}$$

$$\begin{aligned} M_u &= \frac{f_{K\Sigma\Xi}}{m_K} \frac{f_{\eta\Sigma\Sigma}}{m_\eta}\ \tau^a_{ij}\ \frac{1}{u - m^2_\Sigma} \\ &\quad \times \bar{\Xi}_j \not{p}_{K_i} (m_\Sigma - \not{q}_u) \not{p}_{\eta} \Sigma^a, \end{aligned} \tag{11}$$

$$\begin{aligned} M_s &= \frac{f_{K\Sigma\Xi}}{m_K} \frac{f_{\eta\Xi\Xi}}{m_\eta}\ \tau^a_{ij}\ \frac{1}{s - m^2_\Xi} \\ &\quad \times \bar{\Xi}_j \not{p}_{\eta} (m_\Xi - \not{q}_s) \not{p}_{K_i} \Sigma^a. \end{aligned} \tag{12}$$

5) $\bar{K}\Lambda \to \bar{K}\Lambda$:

$$\begin{aligned} M_t = &\left[g_{\omega KK} g^t_{\omega\Lambda\Lambda} \frac{g^{\mu\nu} - q_t^\mu q_t^\nu / m^2_\omega}{t - M^2_\omega} \right. \\ &\left. +\ g_{\phi KK} g^t_{\phi\Lambda\Lambda} \frac{g^{\mu\nu} - q_t^\mu q_t^\nu / m^2_\phi}{t - M^2_\phi} \right] \\ &\times \delta_{ij}\ (p_{K_i\mu} + p_{K_j\mu}) \\ &\times \bar{\Lambda} \left[\gamma_\nu - \frac{p_{\Lambda\nu} + p'_{\Lambda\nu}}{2m_\Lambda} \right] \Lambda, \end{aligned} \tag{13}$$

$$\begin{aligned} M_u &= \frac{f_{KN\Lambda}}{m_K} \frac{f_{KN\Lambda}}{m_K}\ \delta_{ij}\ \frac{1}{u - m^2_N} \\ &\quad \times \bar{\Lambda} \not{p}_{K_i} (m_N - \not{q}_u) \not{p}_{\bar{K}_j} \Lambda, \end{aligned} \tag{14}$$

$$\begin{aligned} M_s &= \frac{f_{K\Lambda\Xi}}{m_K} \frac{f_{K\Lambda\Xi}}{m_K}\ \delta_{ij}\ \frac{1}{s - m^2_\Xi} \\ &\quad \times \bar{\Lambda} \not{p}_{K_j} (m_\Xi - \not{q}_s) \not{p}_{K_i} \Lambda. \end{aligned} \tag{15}$$

6) $\bar{K}\Sigma \to \bar{K}\Sigma$:

$$\begin{aligned} M_t &= g_{\rho KK} g_{\rho\Sigma\Sigma}\ i\epsilon^{abc}\tau^c_{ij}\ (p_{K_i\mu} + p_{K_j\mu}) \\ &\quad \times \frac{g^{\mu\nu} - q_t^\mu q_t^\nu / m^2_\rho}{t - m^2_\rho} \\ &\quad \times \bar{\Sigma}_a \left[(1+\kappa)\gamma_\nu - \kappa \frac{p_{\Sigma^a\nu} + p_{\Sigma^b_\nu}}{2m_\Sigma} \right] \Sigma_b \\ &\quad + g_{\omega KK} g^t_{\omega\Sigma\Sigma} \delta_{ij}\delta_{ab} (p_{K_i\mu} + p_{K_j\mu}) \\ &\quad \times \frac{g^{\mu\nu} - q_t^\mu q_t^\nu / m^2_\omega}{t - m^2_\omega} \\ &\quad \times \bar{\Sigma}_a \left[\gamma_\nu - \frac{p_{\Sigma_a\nu} + p_{\Sigma_b\nu}}{2m_\Sigma} \right] \Sigma_b, \end{aligned} \tag{16}$$

$$\begin{aligned} M_u &= \frac{f_{KN\Sigma}}{m_K} \frac{f_{KN\Sigma}}{m_K}\ (\tau^a\tau^b)_{ij}\ \frac{1}{u - m^2_N} \\ &\quad \times \bar{\Sigma}_a \not{p}_{K_i} (m_N - \not{q}_u) \not{p}_{K_j} \Sigma_b, \end{aligned} \tag{17}$$

$$\begin{aligned} M_s &= \frac{f_{K\Sigma\Xi}}{m_K} \frac{f_{K\Sigma\Xi}}{m_K}\ (\tau^b\tau^a)_{ij}\ \frac{1}{s - m^2_\Xi} \\ &\quad \times \bar{\Sigma}_a \not{p}_{K_j} (m_\Xi - \not{q}_s) \not{p}_{K_i} \Sigma_b. \end{aligned} \tag{18}$$

7) $\pi\Xi \to \pi\Xi$:

$$\begin{aligned}
M_t &= g_{\rho\pi\pi} g_{\rho\Xi\Xi}\ i\epsilon_{abc}\tau^c_{ij}\ (p_{\pi^a\mu} + p_{\pi^b\mu}) \\
&\quad \times \frac{g^{\mu\nu} - q_t^\mu q_t^\nu / m_\rho^2}{t - m_\rho^2} \\
&\quad \times \bar{\Xi}_j \left[(1+\kappa)\gamma_\nu - \kappa \frac{p_{\Xi_f\nu} + p_{\Xi_i\nu}}{2m_\Xi}\right] \Xi_i, && (19) \\
M_u &= \frac{f_{\pi\Xi\Xi}}{m_\pi}\frac{f_{\pi\Xi\Xi}}{m_\pi}\ (\tau^a\tau^b)_{ij}\ \frac{1}{u - m_\Xi^2} \\
&\quad \times \bar{\Xi}_j \not{p}_{\pi^b} (m_\Xi - \not{q}_u) \not{p}_{\pi^a} \Xi_i, && (20) \\
M_s &= \frac{f_{\pi\Xi\Xi}}{m_\pi}\frac{f_{\pi\Xi\Xi}}{m_\pi}\ (\tau^b\tau^a)_{ij}\ \frac{1}{s - m_\Xi^2} \\
&\quad \times \bar{\Xi}_j \not{p}_{\pi^a} (m_\Xi - \not{q}_s) \not{p}_{\pi^b} \Xi_i. && (21)
\end{aligned}$$

8) $\eta\Xi \to \eta\Xi$:

$$\begin{aligned}
M_u &= \frac{f_{\eta\Xi\Xi}}{m_\eta}\frac{f_{\eta\Xi\Xi}}{m_\eta}\ \delta_{ij}\ \frac{1}{u - m_\Xi^2} \\
&\quad \times \bar{\Xi}_j \not{p}_{\eta_i} (m_\Xi - \not{q}_u) \not{p}_{\eta_f} \Xi_i, && (22) \\
M_s &= \frac{f_{\eta\Xi\Xi}}{m_\eta}\frac{f_{\eta\Xi\Xi}}{m_\eta}\ \delta_{ij}\ \frac{1}{s - m_\Xi^2} \\
&\quad \times \bar{\Xi}_j \not{p}_{\eta_f} (m_\Xi - \not{q}_s) \not{p}_{\eta_i} \Xi_i. && (23)
\end{aligned}$$

9) $\bar{K}\Lambda \to \bar{K}\Sigma$:

$$\begin{aligned}
M_t &= g_{\rho KK} g^t_{\rho\Sigma\Lambda}\ \tau^a_{ij}\ (p_{K_i\mu} + p_{K_j\mu}) \\
&\quad \times \frac{g^{\mu\nu} - q_t^\mu q_t^\nu / m_\rho^2}{t - m_\rho^2} \\
&\quad \times \bar{\Sigma}_a \left[\gamma_\nu - \frac{p_{\Sigma_a\nu} + p_{\Lambda\nu}}{m_\Lambda + m_\Sigma}\right] \Lambda, && (24) \\
M_u &= \frac{f_{KN\Sigma}}{m_K}\frac{f_{KN\Lambda}}{m_K}\ \tau^a_{ij}\ \frac{1}{u - m_N^2} \\
&\quad \times \bar{\Sigma}_a \not{p}_{K_i} (m_N - \not{q}_u) \not{p}_{K_j} \Lambda, && (25) \\
M_s &= \frac{f_{K\Lambda\Xi}}{m_K}\frac{f_{K\Sigma\Xi}}{m_K}\ \tau^a_{ij}\ \frac{1}{s - m_\Xi^2} \\
&\quad \times \bar{\Sigma}_a \not{p}_{K_j} (m_\Xi - \not{q}_s) \not{p}_{K_i} \Lambda. && (26)
\end{aligned}$$

10) $\pi\Xi \to \eta\Xi$:

$$\begin{aligned}
M_u &= \frac{f_{\pi\Xi\Xi}}{m_\pi}\frac{f_{\eta\Xi\Xi}}{m_\eta}\ \tau^a_{ij}\ \frac{1}{u - m_\Xi^2} \\
&\quad \times \bar{\Xi}_j \not{p}_{\pi_a} (m_\Xi - \not{q}_u) \not{p}_\eta \Xi_i, && (27) \\
M_s &= \frac{f_{\pi\Xi\Xi}}{m_\pi}\frac{f_{\eta\Xi\Xi}}{m_\eta}\ \tau^a_{ij}\ \frac{1}{s - m_\Xi^2} \\
&\quad \times \bar{\Xi}_j \not{p}_\eta (m_\Xi - \not{q}_s) \not{p}_{\pi_a} \Xi_i. && (28)
\end{aligned}$$

[1] J. Rafelski and B. Müller, Phys. Lett. B **101**, 111 (1982).

[2] B. Zhang, C. M. Ko, B. A. Li, and Z. Lin, Phys. Rev. C **61**, 067901 (2000). Z. Lin, S. Pal, C. M. Ko, B. A. Li, and B. Zhang, *ibid.* **64**, 011902 (2001); Nucl. Phys. A **698**, 375c (2002).

[3] S. Pal, C. M. Ko, and Z. W. Lin., nucl-th/0106073.

[4] C. Cugnon, P. Deneye, and J. Vandermeullen, Phys. Rev. C **41**, 1701 (1990).

[5] A. Baldini *et al.*, *Total Cross Sections of High Energy Particles* (Springer, Heidelberg, 1988).

[6] Z. W. Lin and C. M. Ko, Phys. Rev. C **62**, 034903 (2000).

[7] Z. W. Lin, T. G. Di, and C. M. Ko, Nucl. Phys. A **689**, 965 (2001).

[8] Z. W. Lin and C. M. Ko, J. Phys. G **27**, 617 (2001).

[9] A. D. Lahiff, nucl-th/0110028.

[10] M. Th. Keil, G. Penner, and U. Mosel, Phys. Rev. C **63**, 045202 (2001).

[11] E. E. Salpeter and H. A. Bethe, Phys. Rev. **84** No. 6, 1232 (1951).

[12] T. Feuster and U. Mosel, Phys. Rev. C **58**, 457 (1998); **59**, 460 (1999).

[13] D. E. Groom *et al.*, Particle Data Group, Eur. Phys. J. C **15** 1 (2000).

[14] B. Holzenkamp, K. Holinde, and J. Speth, Nucl. Phys. A **500**, 485 (1989).

[15] R. A. Adelseck and B. Saghai, Phys. Rev. C **42**, 108 (1990).

[16] B. C. Pearce and B. K. Jennings, Nucl. Phys. A **528**, 655 (1991).

[17] T. Ericson and W. Weise, *Pions and Nuclei* (Clarendon Press, Oxford, 1988).

[18] B. H. Bransden and R. G. Morehouse, *The Pion-Nucleon System* (Princeton University Press, 1973).

[19] C. M. Ko, Phys. Lett. B **120**, 294 (1983).

[20] G. Q. Li, C. M. Ko, and X. S. Fang, Phys. Lett. B **329**, 149 (1994).

[21] W. Cassing, E. L. Bratkovskaya, U. Mosel, S. Teis, and A. Sibirtsev, Nucl. Phys. A **614**, 415 (1997).

[22] A. Schöter *et al.*, Z. Phys. A **350**, 101 (1994).

[23] E. Anderson *et al.*, WA97 Collaboration, Phys. Lett. B **433**, 209 (1998); *ibid.* **449**, 401 (1999); J. Phys. G **25**, 171 (1999).

[24] M. F. M. Lutz and E. E. Kolomeitsev, Nucl. Phys. A **700**, 193 (2002).